JOURNAL OF MASS SPECTROMETRY
J. Mass Spectrom. 2005; **40**: 946–954
Published online 2 June 2005 in Wiley InterScience (www.interscience.wiley.com). DOI: 10.1002/jms.872

JMS

Covalent modification of actin by 4-hydroxy-*trans*-2-nonenal (HNE): LC-ESI-MS/MS evidence for Cys374 Michael adduction

Giancarlo Aldini,[1]* Isabella Dalle-Donne,[2] Giulio Vistoli,[1] Roberto Maffei Facino[1] and Marina Carini[1]

[1] Istituto Chimico Farmaceutico Tossicologico, University of Milan, Viale Abruzzi 42, I-20131 Milan, Italy
[2] Dipartimento di Biologia, University of Milan, via Celoria 26, I-20133 Milan, Italy

Received 14 February 2005; Accepted 22 March 2005

We demonstrate for the first time, by a combined mass spectrometric and computational approach, that G- and F-actin can be covalently modified by the lipid-derived aldehyde, 4-hydroxy-*trans*-2-nonenal, providing information on the molecular mass of modified protein and the mechanism and site of adduction.

ESI-MS analysis of actin treated with different molar ratios of HNE (1 : 1 to 1 : 20) showed the formation of a protein derivative in which there was an increase of 156 Da (42028 Da) over native actin (41872 Da), consistent with the adduction of one HNE residue through Michael addition. To identify the site of HNE adduction, G- and F-actin were stabilized by $NaBH_4$ reduction and digested with trypsin. LC-ESI-MS/MS analysis in data-dependent scan mode of the resulting peptides unequivocally indicated that Cys374 is the site of HNE adduction. Computational studies showed that the reactivity of Cys374 residue is due to a significant accessible surface and substantial thiol acidity due to the particular microenvironment surrounding Cys374. Copyright © 2005 John Wiley & Sons, Ltd.

KEYWORDS: actin; 4-hydroxy-*trans*-2-nonenal; Michael adduction; LC-ESI-MS/MS analysis; computational analysis; Cys374 as target residue

INTRODUCTION

Actin is a protein directly involved in the conversion of chemical energy into mechanical work, and the molecule contains ATP as an essential component. Although muscle actin (α isoform) has been the most studied, the protein is widely found in nature and is a structural component of the cytoskeleton (β and γ isoforms) of perhaps of all cell types. The actin cytoskeleton exists in a dynamic steady state, where monomeric actin (G-actin) polymerizes onto the fast-growing ends of actin filaments (F-actin), and depolymerizes off their slow-growing ends.

In many mammalian cells, including hepatocytes, human fibroblasts and platelets, the actin cytoskeleton is one of the earliest targets for attack by reactive oxygen species (ROS)[1] including protein carbonylation. Carbonylation of actin has been shown *in vivo* to affect actin filament dynamics and, consequently, the morphology, contractility, and motility of cells.[1–3] Enhancement of actin carbonylation, causing disruption of the actin cytoskeleton and loss of the barrier function, has been seen in human intestinal cells after exposure to hydrogen peroxide and hypochlorous acid, used as models of oxidant insult.[2,3] A significant specific increase in the actin carbonyl content has been reported in human brain regions severely affected by Alzheimer's disease,[4] in colonic mucosa from patients suffering from inflammatory bowel disease,[5] in post-ischemic isolated rat hearts, associated with significant depression of post-ischemic contractile function,[6,7] and in septic rat diaphragms.[8]

The introduction of carbonyl groups (aldehydes and ketones) into proteins can arise at different sites and by different mechanisms.[9] Carbonyl derivatives are produced by direct reaction of ROS with the side chains of arginine, lysine, proline, and threonine residues. Carbonyls can also be generated through oxidative cleavage of proteins by either the α-amidation pathway or by oxidation of glutamyl side chains, by secondary reaction of the primary amino group of Lys residues with reducing sugars or their advanced glycation end-products (AGEs), and by Michael-addition reaction of cysteine, lysine or histidine residues with intermediate lipoxidation products generated during peroxidation of polyunsaturated fatty acids, such as 2-propenal (acrolein), malondialdehyde (MDA), and 4-hydroxynonenal (HNE).

Although actin carbonylation has been clearly evidenced by slot or Western immunoblot with anti-(2,4-dinitrophenylhydrazone) (DNP) primary antibody, and after 1D- or 2D-electrophoresis,[1–7] the carbonylation mechanism,

*Correspondence to: Giancarlo Aldini, Istituto Chimico Farmaceutico Tossicologico, University of Milan, Viale Abruzzi 42, 20131 Milan, Italy. E-mail: giancarlo.aldini@unimi.it
Contract/grant sponsor: MURST.
Contract/grant sponsor: Cofinanziamento Programma Nazionale 2004-2005.

as well as the sites of carbonyl insertion, still remains unknown.

Since actin contains several nucleophilic sites particularly susceptible to aldehyde adduction (5 Cys, 9 His, and 19 Lys residues), to achieve a better understanding of the molecular basis of carbonylation we investigated whether actin is a target protein for modification by lipid-derived aldehydes. This was done by incubating actin with HNE, one of the most reactive and cytotoxic α,β-unsaturated aldehydes generated by the lipid peroxidation of polyunsaturated fatty acids, and investigating the carbonylation mechanism and the HNE modification sites of the protein by a combined computational and mass spectrometric approach never previously reported for actin.

EXPERIMENTAL

Chemicals

All chemicals and reagents were of analytical grade and purchased from Sigma-Fluka-Aldrich Chemical (Milan, Italy). LC-grade and analytical-grade organic solvents were purchased from Merck (Bracco, Milan, Italy). LC-grade water was prepared with a Milli-Q water purification system (Millipore, Bedford, MA, USA). 4-Hydroxy-non-2-enal diethylacetal (HNE-DEA) was prepared as reported by Rees *et al*.[10] and 4-hydroxy-*trans*-2-nonenal (HNE) by the acid treatment of HNE-DEA (1 mM HCl for 1 h at room temperature) and quantitated by UV spectroscopy (λ max 224 nm; ε13 750 L mol^{-1}cm^{-1}). Sequence-grade modified trypsin was obtained from Promega (Milan, Italy).

Preparation of skeletal muscle actin and HNE exposure

G-actin was prepared from rabbit skeletal muscles according to the method of Spudich and Watt[11] with an additional Sephadex G-150 gel filtration step.[12] G-actin concentration was determined by measuring the absorbance at 290 nm, using an extinction coefficient of 0.63 ml mg^{-1}cm^{-1}. Before use, G-actin solutions were clarified by 60-min centrifugation at 100 000 *g*; protein solutions and buffers were then filtered through 0.20 μm disposable filters and degassed. The experiments were done in buffer containing 2 mM Tris-HCl, pH 7.5, 0.2 mM ATP, 0.2 mM $CaCl_2$, 2 mM NaN_3, unless stated otherwise.

F-actin was prepared by polymerization of G-actin (23.6 μM) at 25 °C by the addition of 100 mM KCl + 2 mM $MgCl_2$ for 18 h. G- and F-actin (23.6 μM as G-actin) were treated with increasing molar ratios of HNE (1 : 1, 1 : 10, 1 : 20) for 120 min at 37 °C, with continuous shaking. Excess of HNE was removed by exhaustive dialysis against Milli-Q. G-actin and F-actin samples were lyophilized under vacuum and stored at −20 °C until MS analysis.

Protein analysis by mass spectrometry

ESI-MS and LC-ESI-MS/MS analyses were done on a Thermo Finnigan LCQ Advantage ion trap mass spectrometer (Thermoquest, Milan Italy).

ESI-MS – Undigested native and HNE-treated G- and F-actin were analyzed by ESI-MS infusion experiments to detect changes in protein mass. Lyophilized protein (250 μg) was dissolved in 200 μl of water, mixed with 200 μl of CH_3CN-H_2O-HCOOH (90 : 10 : 0.4, v/v/v), and infused into the mass spectrometer at a flow-rate of 20 μl min^{-1} under the following instrumental conditions: positive-ion mode, mass range m/z 700–2000; capillary temperature 220 °C; spray voltage applied to the needle 5 kV; capillary voltage 46 V. The flow-rate of the nebulizer gas (nitrogen) was 0.5 L min^{-1}. ESI-MS spectra were deconvoluted using the software package Bioworks 3.1 (Thermoquest, Milan, Italy).

LC-ESI-MS/MS – Tryptic peptide maps were generated by LC-ESI-MS/MS analysis in data-dependent scan mode. For sample preparation, lyophilized target protein (250 μg) was dissolved in 100 μl 50 mM Tris-HCl (pH 8) containing 6 M guanidine HCl and 0.5 M $NaBH_4$. After 60 min at 37 °C, the sample was spiked with β-mercaptoethanol (3 mM final concentration) and heated at 95 °C for 20 min. After denaturation, the sample was diluted to 1 ml with 50 mM Tris-HCl (pH 7.6), 1 mM $CaCl_2$. A 500 μl-aliquot was then digested with trypsin at a protease : protein ratio of 1 : 20 (w/w) for 24 h at 37 °C. To terminate the protease activity, samples were spiked with TCA (10% final concentration), centrifuged at 18 000 rpm for 10 min and 5 μl of the supernatant was injected into a quaternary pump HPLC system (Surveyor LC system, Thermoquest, Milan, Italy). Separations were done by reversed-phase elution with an Agilent Zorbax SB-C18 column (4 mm i.d., particle size 3.5 μm) (CPS Analitica, Milan, Italy) protected by an Agilent Zorbax R-P guard column, thermostated at 25 °C. An 80-min linear gradient from 0 to 60% B was used to elute the digested peptides with phase A (0.1% HCOOH in water) and B (CH_3CN-H_2O-HCOOH; 90 : 10 : 0.1, v/v/v); the mobile phase was delivered at a flow-rate of 0.2 ml min^{-1}. The ESI-MS source was set in positive-ion mode, the capillary temperature at 250 °C, spray voltage 4.5 kV, source current 10 μA, and capillary voltage 10.0 V. The flow-rate of the nebulizer gas (nitrogen) was 5 L min^{-1}. Peptide sequences were identified using the database search software turboSEQUEST (Bioworks 3.1, Thermoquest, Milan, Italy), using a database containing only the protein of interest and assuming trypsin digestion. The protein sequence of α-actin from skeletal muscle was obtained from the SWISS-PROT database (primary accession number P68136), and PEPTIDEMASS[13] was used to calculate theoretical digested masses based on tryptic digest.

Computation methods

The structure of monomeric actin in ATP state was retrieved from the PDB archive (PDB Id: 1NWK).[14] The structure was completed by adding three missing fragments (Asp1 to Thr5, His40 to Asp51 and Arg372 to Phe375) and hydrogen atoms (Arg, Lys, Asp and Glu residues were ionized, while His residues were preserved neutral by default). More specifically, the first fragment (Asp1 to Thr5) was manually constructed in α-helix using the VEGA fragment builder,[15] the second fragment (His40 to Asp51) was added using the corresponding one of the actin in ADP state (PDB code 1J6Z),[16] and the third fragment (Arg372 to Phe375) was added using the corresponding one of the rabbit actin in complex with kabiramide C (PDB code 1QZ5).[17] The AMP

nucleotide was manually transformed in the ATP molecule. These preliminary modifications were made using the VEGA program.[15] The resulting structure was minimized in a two-phase procedure: first without any constraints (apart from the fixed Ca^{++} ions) until root mean square (RMS) = 1 to adjust the conformation of the inserted fragments avoiding bad intramolecular interactions, and then with the backbone fixed until RMS = 0.01 to preserve the experimental folding. A 1-ns molecular dynamics (MD) simulation was carried out with backbone fixed to equilibrate the conformations of the side chains, and the lowest energy structure of this simulation was used to calculate the solvent accessible surface (SAS) per residue and to extract the peptides around the Cys residues. In detail, these fragments were obtained by selecting the residues inside a 2-Å sphere around a cysteine (for example, for Cys374 the selected fragment corresponds to the tetra-peptide Arg372-Lys373-Cys374-Phe375). Their precise atomic charges were calculated with MOPAC6.0 from the corresponding electrostatic potential (keywords, 'AM1', 'PRECISE', '1SCF', 'ESP' and 'MMOK').

The simulations were performed with Namd 2.51,[18] using the CHARMM force field and Gasteiger's atomic charges, and the Ca^{++} ions were always kept fixed. The MD simulation was done with the following characteristics: initial heating from 0 to 300 K over 3000 iterations (3 ps, i.e. 1 K/10 iterations), 1 ns of equilibrating MD with constant temperature of 300 K by means of Langevin's algorithm, and integration of Newton's equation each 1 fs according to Verlet's algorithm. Minimizations were based on the conjugate gradients algorithm. The SAS values were calculated with a solvent probe of radius 1.4 Å.

RESULTS AND DISCUSSION

Target proteins were first analyzed by ESI-MS (infusion experiments) to unequivocally establish the stoichiometry of HNE adduction and to measure the increase in protein

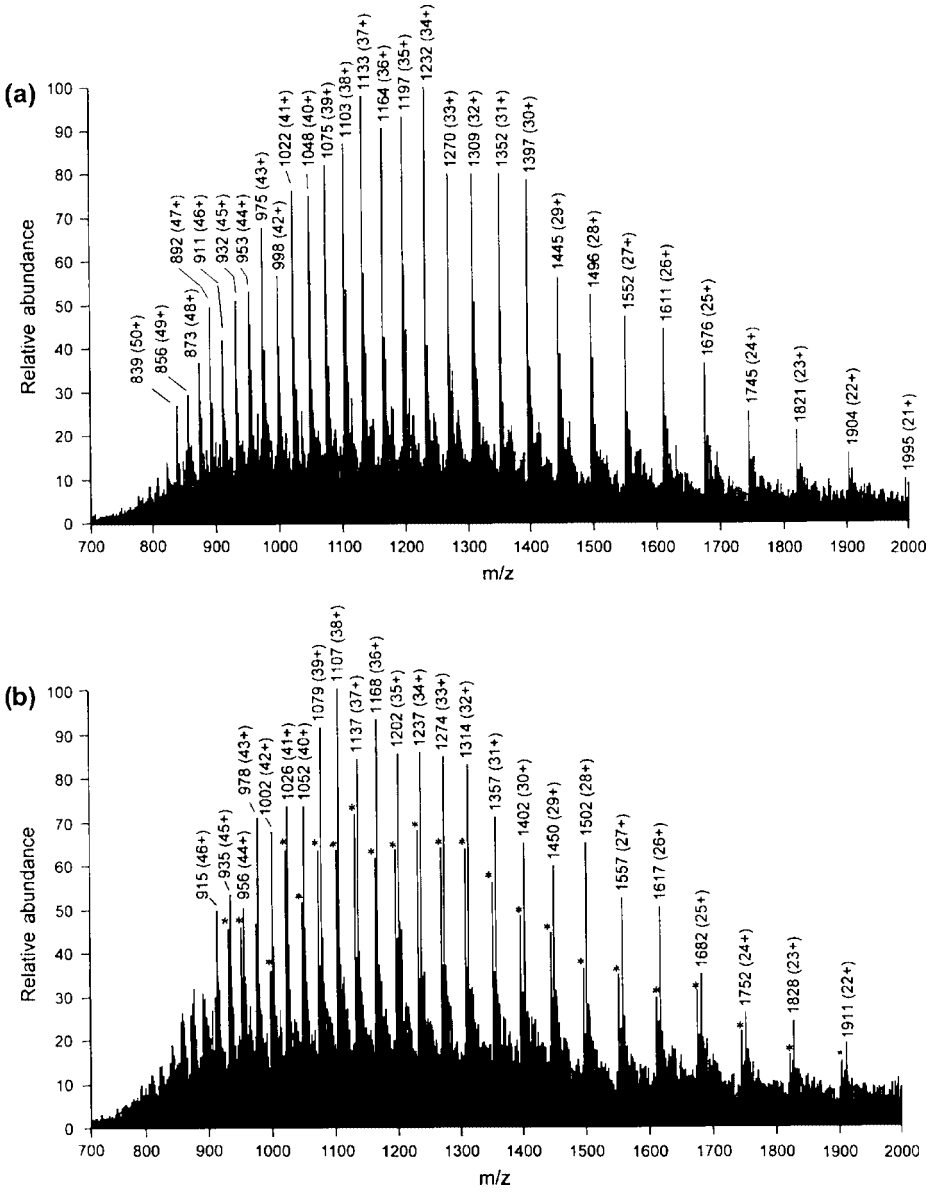

Figure 1. Positive-ion ESI-MS spectra of (a) untreated and (b) HNE-treated actin at a molar ratio of 1 : 10. In spectrum (b), *denotes multiple charged peaks relative to native actin.

mass adduct(s). Figure 1 shows representative ESI-mass spectra of native (a) and HNE-modified (b) G-actin (1 : 10 molar ratio), which were recorded by signal averaging for 10 min, corresponding to the consumption of approximately 3 nmoles protein. The mass spectrum of native actin shows a range of protonation states (a typical feature of ESI for proteins) with multiple charged peaks ranging from m/z 839 to m/z 1995, corresponding to the addition of 50 to 21 protons. The mass spectrum reported in Fig. 1(b) for HNE-treated actin shows, besides the multiple charged peaks of unmodified actin (peaks labeled with an asterisk), a second series of multiple charged peaks with higher abundance, which clearly indicates modification of the actin.

The pattern of adduction and component molecular weights is clearer in the mass deconvoluted spectra shown in Fig. 2: the native G- and F-actin show a MW of 41 872 Da, which corresponds to the theoretical isotope-averaged molecular weight of N-terminal acetylated α-actin with one methylated His residue, as recently determined by FTICR-MS analysis of skeletal muscle actin.[19] When actin (G or F) was incubated with HNE (1 : 1), a distinct peak at 42 028 Da appeared in the deconvoluted spectra, whose intensity significantly increased with the protein : HNE molar ratio, concomitant to a decrease in the peak for native protein (Fig. 2).

These results clearly indicate that: (i) only a mono-HNE adduct is formed under these experimental conditions (2 h

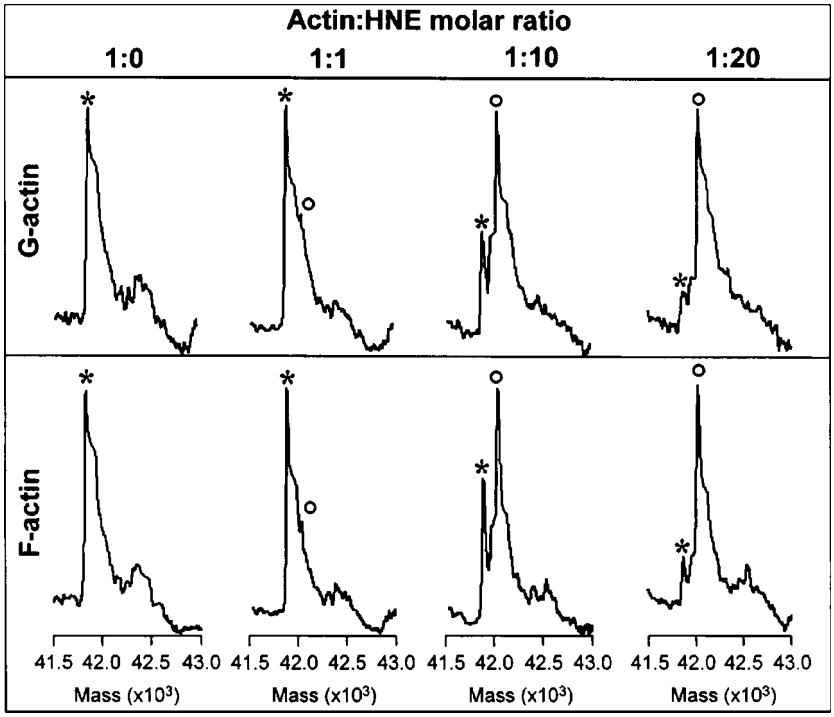

Figure 2. Deconvoluted ESI-mass spectra relative to native and HNE-treated G- and F-actin at molar ratios of 1 : 1, 1 : 10, 1 : 20. *MW = 41 872 Da; ○MW = 42 028 Da.

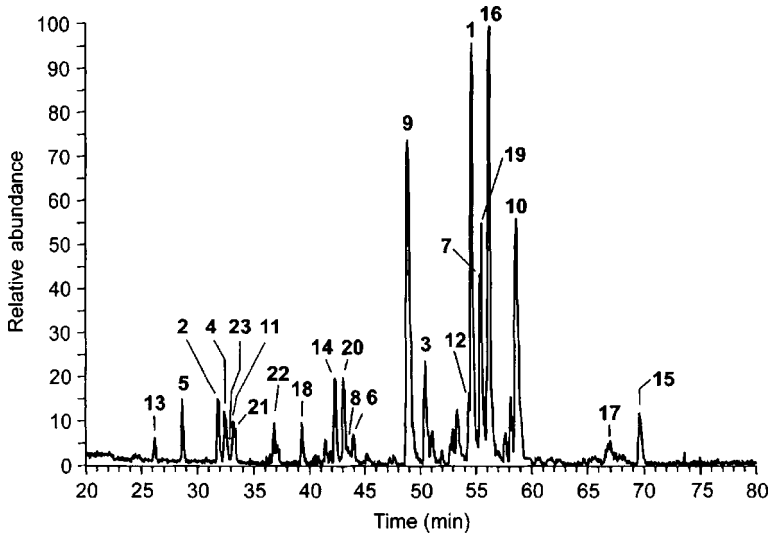

Figure 3. LC-ESI-MS analysis of tryptic peptides from actin. The elution positions of identified tryptic peptides are indicated in the total ion current and summarized in Table 2.

incubation); (ii) the increase of 156 Da in MW confirms the insertion of HNE through a Michael adduction (the theoretical mass increment for the HNE-Michael adduct is 156.22) (iii) both the monomeric and the polymerized forms of actin show similar reactivity and adduction mechanism towards HNE.

As regards the site of HNE adduction, two parameters mainly regulate the adduction chemistry: the nucleophilic reactivity of amino acids and their accessible surface. Actin contains 32 nucleophilic residues (5 Cys, 8 His and 19 Lys) and several of these, as calculated by computational analysis (Table 1), have an accessible surface that is at least 30% of the free amino acid, making them potential sites for HNE adduction (namely, Cys374, His40, His173, Lys113, Lys191, Lys215, Lys238, and Lys326).

To characterize the structural modification of actin by HNE, the native and the HNE-treated actin were digested with trypsin, then analyzed by LC-ESI-MS/MS after $NaBH_4$ reduction, an established procedure for adduct stabilization.[20,21] Peptide mass mapping (Fig. 3) of native actin provided identification of the peptides accounting for approximately 78% of the protein sequence (Table 2). This sequence analysis confirms the N-terminal acetylation in Asp1 and His73 as a methylated residue (peak 7). Cys residues are present as disulfides with the reducing agent β-mercaptoethanol.

Since the order of reactivity of the nucleophilic amino acids towards HNE is Cys $\gg$ His $>$ Lys[22] and the most accessible residue is Cys374, as a first step we searched for HNE-modified Cys-containing peptides. This was done by neutral loss scan analysis of the HNE-adducted tryptic mixture by scanning for the neutral loss of m/z 158, 79 and 53, corresponding to the loss of a neutral reduced HNE moiety from singly, doubly and triply charged precursors. This procedure was of limited analytical utility in the case of HNE-modified His peptides,[23] but proved particularly suited for HNE-modified Cys peptides, since their typical MS/MS fragmentation pattern is characterized by a retro-Michael reaction, as for GSH-HNE adducts.[10,24]

Figure 4 shows the map for the selected neutral loss mass of 158 Da, relative to the tryptic peptides of native (a) and HNE-treated actin (b). These reconstructed spectra consist of all the parent ions that gave products within the neutral loss of 158 Da ($\pm$1 tolerance). Both spectra are characterized by several parent ions and differ only in the presence of the precursor ion at m/z 427 in digested, modified actin, corresponding to the $[M + H]^+$ of the HNE-adducted Cys374-Phe375 dipeptide. The MS/MS spectrum of the $[M + H]^+$ ion at m/z 427 (Fig. 5) contains, besides the $[M + H - H_2O]^+$ ion at m/z 409, the typical retro-Michael ion fragment at m/z 269 $[M + H - 158]^+$ and the corresponding fragment ion due to loss of NH_3 (m/z 252). The presence of the HNE-adducted b ion at m/z 262 unequivocally indicates that the HNE-Michael adduct is associated with Cys374.

Confirmation is obtained by recording the selected ion current (SIC) for the $[M + H]^+$ ion of the unmodified Cys374-Phe375 dipeptide at m/z 345 (as disulfide with the reducing agent β-mercaptoethanol): the peak at 32.6 min relative to the Cys374-Phe375 dipeptide is present only in digested native actin, not in HNE-treated actin (Fig. 6). Conversely, the SIC of the ion at m/z 427 shows four distinct peaks with retention times (RT) between 60 and 62 min, which are present only in the digested HNE-treated actin, and are attributed to the four diasteroisomers of the HNE-Cys374-Phe375 adduct. Formation of these isomers is explained by considering that nucleophilic addition of the thiol group of Cys374 to C3 of a racemic mixture of HNE, followed by $NaBH_4$ reduction, generates a Michael adduct diol derivative (Fig. 6), bearing two chiral carbons beside the two fixed centers (*R*)Cys and (*S*)Phe (four

Table 1. SAS values for the nucleophilic reactive residues of actin

Residue	SAS (Å^2)	SAS %[a]
Cys free	**256.4**	–
Cys10	0	0.0
Cys217	0.7	0.3
Cys257	0	0.0
Cys285	0.4	0.2
Cys374[b]	106.2	41.5
His free	**320.1**	–
His40[b]	122.2	38.2
His87	85.6	26.7
His88	38.3	12.0
His101	4.5	1.4
His161	0	0.0
His173[b]	117.4	36.7
His275	30.7	9.6
His371	45.5	14.2
Lys free	**341.6**	–
Lys18	0.5	0.1
Lys50	76.9	22.5
Lys61	60.8	17.8
Lys68	47.5	13.9
Lys84	53.6	15.7
Lys113[b]	123.6	36.2
Lys118	83.6	24.5
Lys191[b]	108.9	31.9
Lys213	0.2	0.1
Lys215[b]	111.5	32.6
Lys238[b]	106.8	31.3
Lys284	82.2	24.1
Lys291	101.3	29.7
Lys315	64.8	19.0
Lys326[b]	132.1	38.7
Lys328	96.6	28.3
Lys336	37.7	11.0
Lys359	71.4	20.9
Lys373	70.1	20.6

[a] Calculated in relation to the free amino acid.

[b] Denotes residues with SAS values $\geq$30% of the corresponding free amino acid.

Table 2. Peptides identified by ESI-LC-MS/MS from native actin

Mass (obs.)	Mass (calc.)[a]	Sequence position	Sequence	Peak no.
1983.9	1984.0	1–18	D[c] EDETTALVC[b] DNGSGLVK	1
975.4	976.0	19–28	AGFAGDDAPR	2
945.8	945.1	29–37	AVFPSIVGR	3
1171.0	1171.4	40–50	HQGVMVGMGQK	4
1197.8	1198.2	51–61	DSYVGDEAQSK	5
643.4	643.8	63–68	GILTLK	6
1975.7	1975.2	69–84	YPIEH[d] GIITNWDDMEK	7
1515.4	1515.7	85–95	IWHHTFYNELR	8
1956.2	1956.2	96–113	VAPEEHPTLLTEAPLNPK	9
2726.3	2726.0	148–173	TTGIVLDSGDGVTHNVPIYEGYALPH	10
643.5	643.7	178–183	LDLAGR	11
997.6	998.1	184–191	DLTDYLMK	12
630.5	630.7	192–196	ILTER	13
1129.9	1130.2	197–206	GYSFVTTAER	14
2555.1	2555.7	216–238	LC[b] YVALDFENEMATAASSSSLEK	15
1790.8	1790.9	239–254	SYELPDGQVITIGNER	16
3208.1	3208.5	257–284	C[b] PETLFQPSFIGMESAGIHETTYNSIMK	17
809.3	809.8	285–290	C[b] DIDIR	18
2246.0	2246.5	292–312	DLYANNVMSGGTTMYPGIADR	19
1161.0	1161.4	316–326	EITALAPSTMK	20
794.5	794.9	329–335	IIAPPER	21
1500.4	1500.6	360–372	QEYDEAGPSIVHR	22
344.0	344.3	374–375	C[b] F	23

[a] Average MW.

[b] Disulfide with the reducing agent β-mercaptoethanol.

[c] N-acetyl derivative.

[d] Methyl derivative; sequence coverage 78%.

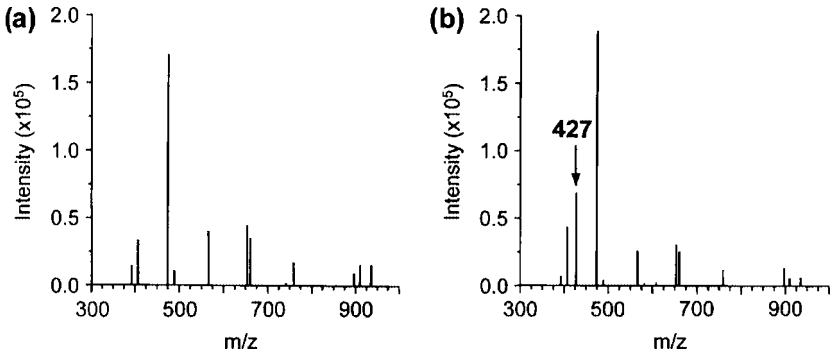

Figure 4. Reconstructed neutral loss spectra showing all the parent ions that produced products within the neutral loss of 158 Da (±1 tolerance) relative to the tryptic peptides from (a) untreated and (b) HNE-treated actin (1 : 20 molar ratio). The spectra differ only in the presence of the precursor ion at *m/z* 427 (arrow) in digested modified actin, corresponding to the $[M + H]^+$ of the HNE-adducted Cys374-Phe375 dipeptide.

diasteroisomers, namely: (3*R*,4*R*)-(*R*)Cys-(*S*)Phe; (3*S*,4*S*)-(*R*)Cys-(*S*)Phe; (3*R*,4*S*)-(*R*)Cys-(*S*)Phe; (3*S*,4*R*)-(*R*)Cys-(*S*)Phe).

The data obtained agree well with those in the literature reporting that the sulfhydryl group of Cys374 in actin is highly accessible and reactive and that Cys374 is the most preferred target of oxidation. In particular, it has been found that Cys374 is the site of the oxidative modification induced by tert-butyl hydroperoxide,[25] it is chemically modified by different agent such as N-ethylmaleimide,[26] (iodoacetamido)-tetramethylrhodamine,[26] or fluorescent dyes,[27,28] and it is specifically involved in the S-nitrosylation[29] and S-glutathionylation reaction.[30]

The specific carbonylation at Cys374, as well as the structural elements that favor the adduction and make the other nucleophilic sites less reactive, can be explained by considering both steric and electronic factors. Table 3 indicates that Cys374 is the unique cysteine that simultaneously possesses both a significant accessible surface and a noteworthy

acidity of S-H bond, as indicated by both the polarity of S-H bond and the stability of corresponding sulphur anion. The atomic charges of the thiol group range from −0.02 (S) and 0.04 (H) in free cysteine to −0.14 (S) and 0.10 (H) in Cys374 (Table 3) and this significant acidity can be explained considering that side chain of Cys374 is closely surrounded by polar residues (such as Arg372). Arg372 and Phe375 raise the acidity of the cysteine thiol group by stabilizing the corresponding sulfur anion, arginine by means of a salt bridge, and phenylalanine by means of an anion-π interaction that involves the sulfur lone pairs.[31] The thiol group of Cys257 also shows significant polarity, but its accessibility is virtually nil.

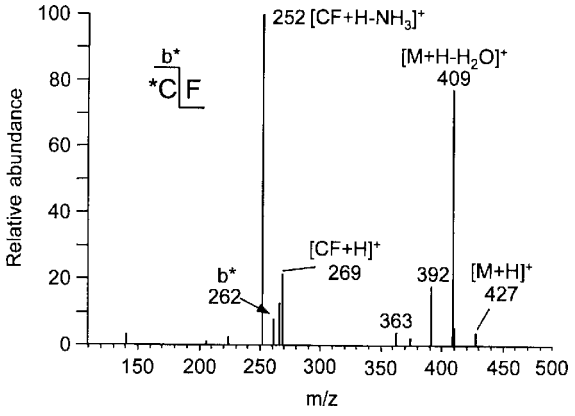

Figure 5. CID mass spectra of the ion *m/z* 427 originating from the tryptic digestion of HNE-adducted actin. Modified fragment ions are labeled with an asterisk and according to the nomenclature of Biemann.[36] The peptide sequence is represented in the one-letter code nomenclature.

Table 3. SAS and polarity of the S−H bond of actin Cys residues

Residue	SAS (Å^2)	q_H	q_S
Cys Free	263.2	+0.04	−0.02
Cys10	0.0	+0.05	−0.07
Cys217	0.7	+0.03	−0.01
Cys257	0.0	+0.10	−0.18
Cys285	0.4	+0.02	−0.05
Cys374	106.2	+0.10	−0.14

CONCLUSIONS

Carbonylation of actin has been detected in several pathological situations by conventional immunochemical and immunohistochemical techniques, which, although furnishing qualitative and quantitative evidence of the process, do not provide information on the mechanism and site. MS-based techniques play a key role in the study of the kinetics and mechanisms of reactive aldehyde-protein interactions,[32,33] providing information on the molecular mass of modified protein and helping estimate the stoichiometry of the reaction (complete structure assignment of protein-HNE adducts is generally obtained by trypsin digestion followed by peptide mass mapping, mainly by HPLC-ESI-MS/MS techniques). The emerging potential of these techniques notwithstanding, no studies have yet investigated whether actin can be covalently modified by lipid-derived aldehydes, such as HNE.

The present findings provide the first evidence that both monomeric and polymeric actin are extremely sensitive to HNE-Michael adduction because of the high reactivity of Cys374, suggesting that this mechanism may be responsible for actin carbonylation detected *in vivo*. In addition, the

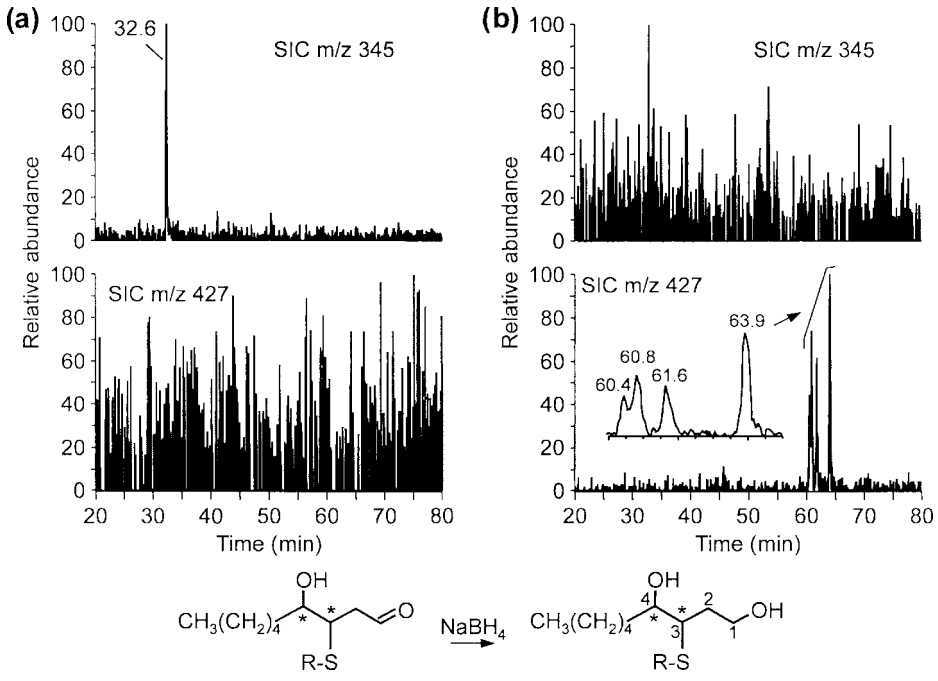

Figure 6. LC-ESI-MS analysis (SICs) of native (a) and HNE-modified (b) actin. SICs are relative to the ions at *m/z* 345 (upper panels) and *m/z* 427 (lower panels).

computational analysis suggests it may be possible to rationalize (or predict) the carbonylation adducts on the basis of both structural and electronic properties of possible reactive residues. It is important to stress that with 2 h incubation (longer incubation times were not explored to avoid excessive actin aggregation, favored by incubation at 37 °C in the absence of reducing agents) the protein was quantitatively modified by HNE molecule (molar ratio 1 : 20), suggesting carbonylation is extremely rapid. However, we cannot exclude that in other conditions (prolonged incubation times or in biological systems) other reactive and accessible nucleophilic residues on actin (such as His40, His173, Lys113, Lys191, Lys215, Lys238, and Lys326) may react with additional HNE molecules.

HNE-modified proteins in isolated rat hearts during ischemia/reperfusion were detected and quantitated using an antibody to HNE-Cys/His/Lys and densitometry of Western blots.[34] Most of the HNE adduct signal was in the cell membrane, but HNE immunofluorescence also showed longitudinal striations with possible co-localization with the myofibrils, suggesting modification of contractile proteins. In addition, using ventricular myocytes isolated from adult male rats, it was recently demonstrated that HNE inhibits cardiac myocyte contraction.[35]

Because this evidence suggests that the myofilaments may also be an important target for oxidant stress during ischemia-reperfusion and that myofilament dysfunction may be related to the formation of HNE adducts with key contractile proteins, studies are in progress in our laboratories to evaluate the effects of HNE carbonylation on actin function *in vitro* and *in vivo*, and to demonstrate actin-HNE adduct formation by mass spectrometric techniques in cell lines, isolated tissues/organs exposed to free radicals, or in the experimental animal under conditions that mimic pathological situations where HNE is massively involved, e.g. ischemia/reperfusion damage as a model of cardiovascular diseases. It must, in any event, be borne in mind that actin carbonylation *in vivo* could also result from mechanisms other than HNE-Michael addition. Our investigations in this field have really just begun.

Acknowledgements

This work was supported by MURST grants (Cofinanziamento Programma Nazionale 2004-2005).

REFERENCES

1. Dalle-Donne I, Rossi R, Milzani A, Di Simplicio P, Colombo R. The actin cytoskeleton response to oxidants: from small heat shock protein phosphorylation to changes in the redox state of actin itself. *Free Radic. Biol. Med.* 2001; **31**: 1624.
2. Banan A, Zhang Y, Losurdo J, Keshavarzian A. Carbonylation and disassembly of the F-actin cytoskeleton in oxidant-induced barrier dysfunction and its prevention by epidermal growth factor and transforming growth factor alpha in a human colonic cell line. *Gut* 2000; **46**: 830.
3. Banan A, Fitzpatrick L, Zhang Y, Keshavarzian A. OPC-compounds prevent oxidant-induced carbonylation and depolymerization of the F-actin cytoskeleton and intestinal barrier hyperpermeability. *Free Radic. Biol. Med.* 2001; **30**: 287.
4. Aksenov MY, Aksenova MV, Butterfield DA, Geddes JW, Markesbery WR. Protein oxidation in the brain in Alzheimer's disease. *Neurosci.* 2001; **103**: 373.
5. Keshavarzian A, Banan A, Farhadi A, Komanduri S, Mutlu E, Zhang Y, Fields JZ. Increases in free radicals and cytoskeletal protein oxidation and nitration in the colon of patients with inflammatory bowel disease. *Gut* 2003; **52**: 720.
6. Powell SA, Gurzenda EM, Wahezi SE. Actin is oxidized during myocardial ischemia. *Free Radic. Biol. Med.* 2001; **30**: 1171.
7. Canton M, Neverova I, Menabo R, Van Eyk J, Di Lisa F. Evidence of myofibrillar protein oxidation induced by postischemic reperfusion in isolated rat hearts. *Am. J. Physiol. Heart Circ. Physiol.* 2004; **286**: H870.
8. Barreiro E, Gea J, Di Falco M, Kriazhev L, James S, Hussain SN. Protein carbonyl formation in the diaphragm. *Am. J. Respir. Cell Mol. Biol.* 2005; **32**: 9.
9. Stadtman ER, Levine RL. Free radical-mediated oxidation of free amino acids and amino acid residues in proteins. *Amino Acids* 2003; **25**: 207.
10. Rees MS, van Kuijk FJGM, Siakotos AN, Mundy BP. Improved synthesis of various isotope labelled 4-hydroxyalkenals and peroxidation intermediates. *Synth. Commun.* 1995; **25**: 3225.
11. Spudich JA, Watt S. The regulation of rabbit skeletal muscle contraction. I. Biochemical studies of the interaction of the tropomyosin-troponin complex with actin and the proteolytic fragments of myosin. *J. Biol. Chem.* 1971; **246**: 4866.
12. MacLean-Fletcher S, Pollard TD. Identification of a factor in conventional muscle actin preparations which inhibits actin filament self-association. *Biochem. Biophys. Res. Commun.* 1980; **96**: 18.
13. Wilkins MR, Lindskog I, Gasteiger E, Bairoch A, Sanchez JC, Hochstrasser DF, Appel RD. Detailed peptide characterisation using PEPTIDEMASS – a World-Wide Web accessible tool. *Electrophoresis* 1997; **18**: 403.
14. Graceffa P, Dominguez R. Crystal structure of monomeric actin in the ATP state. Structural basis of nucleotide-dependent actin dynamics. *J. Biol. Chem.* 2003; **278**: 34 172.
15. Pedretti A, Villa L, Vistoli G. VEGA: a versatile program to convert, handle and visualize molecular structure on Windows-based PCs. *J. Mol. Graph. Model.* 2002; **21**: 47.
16. Otterbein LR, Graceffa P, Dominguez R. The crystal structure of uncomplexed actin in the ADP state. *Science* 2001; **293**: 708.
17. Klenchin VA, Allingham JS, King R, Tanaka J, Marriott G, Rayment I. Trisoxazole macrolide toxins mimic the binding of actin-capping proteins to actin. *Nat. Struct. Biol.* 2003; **10**: 1058.
18. Kalè L, Skeel R, Bhandarkar M, Brunner R, Gursoy A, Krawetz N, Phillips J, Shinozaki A, Varadarajan K, Schulten K. NAMD2: Greater scalability for parallel molecular dynamics. *J. Comput. Phys.* 1999; **151**: 283.
19. Bergen HR, Ajtai K, Burghardt TP, Nepomuceno AI, Muddiman DC. 3rd. Mass spectral determination of skeletal/cardiac actin isoform ratios in cardiac muscle. *Rapid Commun. Mass Spectrom.* 2003; **17**: 1467.
20. Crabb JW, O'Neil J, Miyagi M, West K, Hoff HF. Hydroxynonenal inactivates cathepsin B by forming Michael adducts with active site residues. *Protein Sci.* 2002; **11**: 831.
21. Fenaille F, Guy PA, Tabet JC. Study of protein modification by 4-hydroxy-2-nonenal and other short-chain aldehydes analyzed by electrospray ionization tandem mass spectrometry. *J. Am. Soc. Mass Spectrom.* 2003; **14**: 215.
22. Doorn JA, Petersen DR. Covalent adduction of nucleophilic amino acids by 4-hydroxynonenal and 4-oxononenal. *Chem. Biol. Interact.* 2003; **143–144**: 93.
23. Bolgar MS, Gaskell SJ. Determination of the sites of 4-hydroxy-2-nonenal adduction to protein by electrospray tandem mass spectrometry. *Anal. Chem.* 1996; **68**: 2325.
24. Aldini G, Granata P, Carini M. Detoxification of cytotoxic α,β-unsaturated aldehydes by carnosine: characterization of conjugated adducts by electrospray ionization tandem mass spectrometry and detection by liquid chromatography/mass spectrometry in rat skeletal muscle. *J. Mass Spectrom.* 2002; **37**: 1219.
25. Dalle-Donne I, Milzani A, Colombo R. The t-butyl hydroperoxide-induced oxidation of actin Cys-374 is coupled with

structural changes in distant regions of the protein. *Biochemistry* 1999; **38**: 12 471.
26. Tait JF, Frieden C. Chemical modification of actin. Acceleration of polymerization and reduction of network formation by reaction with N-ethylmaleimide, (iodoacetamido) tetramethylrhodamine, or 7-chloro-4-nitro-2,1,3-benzoxadiazole. *Biochemistry* 1982; **21**: 6046.
27. Yasunaga T, Wakabayashi T. Relocation of Cys374 of actin induced by labeling with fluorescent dyes. *J. Biochem. (Tokyo)* 2001; **129**: 201.
28. Crosbie RH, Miller C, Cheung P, Goodnight T, Muhlrad A, Reisler E. Structural connectivity in actin: effect of C-terminal modifications on the properties of actin. *Biophys. J.* 1994; **67**: 1957.
29. Dalle-Donne I, Milzani A, Giustarini D, Di Simplicio P, Colombo R, Rossi R. S-NO-Actin: S-nitrosylation kinetics and effect on vascular smooth muscle. *J. Muscle Res. Cell Motil.* 2000; **21**: 171.
30. Dalle-Donne I, Giustarini D, Rossi R, Colombo R, Milzani A. Reversible S-glutathionylation of Cys(374) regulates actin filament formation by inducing structural changes in the actin molecule. *Free Radic. Biol. Med.* 2003; **34**: 23.
31. Garau C, Frontera A, Quinonero D, Ballester P, Costa A, Deya PM. Cation-pi versus anion-pi interactions: energetic, charge transfer, and aromatic aspects. *J. Phys. Chem. A* 2004; **108**: 9423.
32. Carini M, Aldini G, Maffei Facino R. Mass spectrometry for detection of 4-hydroxy-trans-2-nonenal (HNE) adducts with peptides and proteins. *Mass Spectrom. Rev.* 2004; **23**: 281.
33. Dalle-Donne I, Scaloni A, Giustarini D, Cavarra E, Tell G, Lungarella G, Colombo R, Rossi R, Milzani A. Proteins as biomarkers of oxidative/nitrosative stress in diseases: The contribution of redox proteomics. *Mass Spectrom. Rev.* 2005; **24**: 55.
34. Eaton P, Li JM, Hearse DJ, Shattock MJ. Formation of 4-hydroxy-2-nonenal-modified proteins in ischemic rat heart. *Am. J. Physiol.* 1999; **276**: H935.
35. Aberle NS 2nd Sr., Picklo MJ, Amarnath V, Ren J. Inhibition of cardiac myocyte contraction by 4-hydroxy-trans-2-nonenal. *Cardiovasc. Toxicol.* 2004; **4**: 21.
36. Biemann K. Contributions of mass spectrometry to peptide and protein structure. *Biomed. Environ. Mass Spectrom.* 1988; **16**: 99.